Total and differential cross-sections for the pp → ppη' reaction near threshold

A. Khoukaz[1,a], I. Geck[1], C. Quentmeier[1], H.-H. Adam[1], A. Budzanowski[2], R. Czyżykiewicz[3], D. Grzonka[4], L. Jarczyk[3], K. Kilian[4], P. Kowina[4,5], N. Lang[1], T. Lister[1], P. Moskal[3,4], W. Oelert[4], C. Piskor-Ignatowicz[3], T. Rożek[5], R. Santo[1], G. Schepers[4], T. Sefzick[4], S. Sewerin[4], M. Siemaszko[5], J. Smyrski[3], A. Strzałkowski[3], A. Täschner[1], P. Winter[4], M. Wolke[4], P. Wüstner[4], and W. Zipper[5]

[1] Institut für Kernphysik, Westfälische Wilhelms-Universität, D-48149 Münster, Germany
[2] Institute of Nuclear Physics, PL-31-342 Cracow, Poland
[3] Institute of Physics, Jagellonian University, PL-30-059 Cracow, Poland
[4] IKP and ZEL, Forschungszentrum Jülich, D-52425 Jülich, Germany
[5] Institute of Physics, University of Silesia, PL-40-007 Katowice, Poland

Abstract. The η'-meson production in the reaction $pp \rightarrow pp\eta'$ has been studied at excess energies of $Q = 26.5$, 32.5 and 46.6 MeV using the internal beam facility COSY-11 at the cooler synchrotron COSY. The total cross-sections as well as one angular distribution for the highest Q-value are presented. The excitation function of the near-threshold data can be described by a pure s-wave phase space distribution with the inclusion of the proton-proton final-state interaction and Coulomb effects. The obtained angular distribution of the η'-mesons is also consistent with pure s-wave production.

PACS. 13.60.Le Meson production – 13.75.-n Hadron-induced low- and intermediate-energy reactions and scattering (energy ≤ 10 GeV) – 13.85.Lg Total cross-sections – 25.40.-h Nucleon-induced reactions

1 Introduction

Measurements on the production of η'-mesons, the heaviest representative of the multiplet of pseudoscalar mesons, allow to study the properties and the structure of this isoscalar meson, which are still far from being well known. Since states with the same quantum numbers IJ^P can mix, the physically observable particles η and η' are considered to be mixed states of the $I = 0$ members of the ground-state pseudoscalar octet and singlet, commonly denoted as η_8 and η_1. In case of an ideal mixing, the η-meson would have a pure non-strange content $(u\bar{u}+d\bar{d})$, while the η' would show up as a pure $s\bar{s}$ state, corresponding to a mixing angle of $\theta_{\mathrm{ideal}} = -\arctan\sqrt{2} \approx -54.7°$. This value is in contrast to the experimentally still inaccurately determined mixing angle θ_P, which has been subject of several investigations [1–12] and was found to be between $-9°$ and $-20°$.

Furthermore, studies on the production of η'-mesons are also important with respect to still controversially discussed topics like possible $c\bar{c}$ or gluonic components in the structure of the η'-meson [8,13–19] or the understanding of the unexpected high mass, which is discussed in the context of the $U(1)_A$ anomaly [17,20,21]. The gluonic contribution to the cross-section for the $NN \rightarrow NN\eta'$ reaction may be inferred by the comparison of the η' production in different isospin channels [18,19,22].

Recently, detailed measurements on the η'-meson production in the reaction channel $pp \rightarrow pp\eta'$ have been performed in the previously unexplored region close to threshold up to an excess energy of $Q = 24$ MeV [23–26] as well at a higher excess energy of $Q = 144$ MeV [27]. In this publication, we present new results on this reaction channel at intermediate excess energies of $Q = 26.5$, 32.5 and 46.6 MeV, filling the gap between the available data sets.

Due to the small relative momenta of the ejectiles in the region of low excess energies, only partial waves of the lowest order participate in the exit channel. Therefore, total- and differential-cross-section data yield nearly unscreened information on relevant production mechanisms and allow to study final-state interactions (FSI) of the participating particles. Consequently, these new data became subject of several model calculations and comparisons with the related reaction channels on the π^0- and η-meson production [28–30].

[a] e-mail: khoukaz@uni-muenster.de

In contradistinction to the corresponding η-meson production channel, whose production amplitude is assumed to be dominated by the excitation of the S_{11} nucleon resonance $N^*(1535)$, the relevance of possible production diagrams to describe the η'-meson formation is still controversially discussed. A prediction for both the shape and the absolute scale of the near-threshold excitation function of the η' production via the reaction $pp \to ppX$ has been determined by Hibou *et al.* [23], comparing the $pp\eta$ and $pp\eta'$ channels within a one-pion exchange model and adjusting an overall normalization factor to fit the $pp\eta$ total-cross-section data. The obtained prediction for the shape of the η' excitation function is able to describe the data well. However, the absolute scale of the total cross-sections is underestimated by a factor of 2-3 by these calculations, which might be interpreted as a signal for the relevance of exchange diagrams of heavier mesons (*e.g.*, ρ) [23] or the importance of the gluonic contact term in the η' production [19].

On the contrary, model calculations by Sibirtsev *et al.* [31], also based on the one-pion exchange diagram including the proton-proton final-state interaction, have been found to be able to describe both the shape as well as the absolute scale of the near-threshold total-cross-section data. This result is argued to indicate either only negligible contributions of the exchange of heavier mesons or a mutual cancellation of their contributions. It should be noted that in both models contributions of initial-state interactions of both protons have been neglected, which have been reported to scale the absolute size of the total cross-sections by a factor of $f = 0.2$ [32] and $f = 0.33$ [33] in the near-threshold region for the η- and η'-mesons, respectively.

Recently, the η'-meson production has been investigated theoretically by Nakayama *et al.* [33] within a relativistic meson exchange model, considering the exchange of π-, η-, ρ-, ω-, σ-, a_0-mesons and including effects of the proton-proton initial- and final-state interaction. These calculations include contributions of nucleonic and mesonic currents as well as contributions of nucleon resonances, denoted as $S_{11}(1897)$ and $P_{11}(1986)$, which have been observed in multipole analyses of η' photoproduction experiments off protons [34]. Though the nucleonic and the mesonic currents are found to reproduce the observed cross-sections, also contributions of the $S_{11}(1897)$-resonance alone are reported to be sufficient to describe the data. However, to determine the relative magnitude of these currents, total- and differential-cross-section data at higher excess energies are needed.

2 Experiment

Measurements on the reaction $pp \to pp\eta'$ have been performed at the internal beam facility COSY-11 [35] at COSY-Jülich [36], using a hydrogen cluster target [37] in front of a COSY-dipole magnet, acting as a magnetic spectrometer. Tracks of positively charged particles, detected in a set of two drift chambers (DC1 and DC2, fig. 1), can
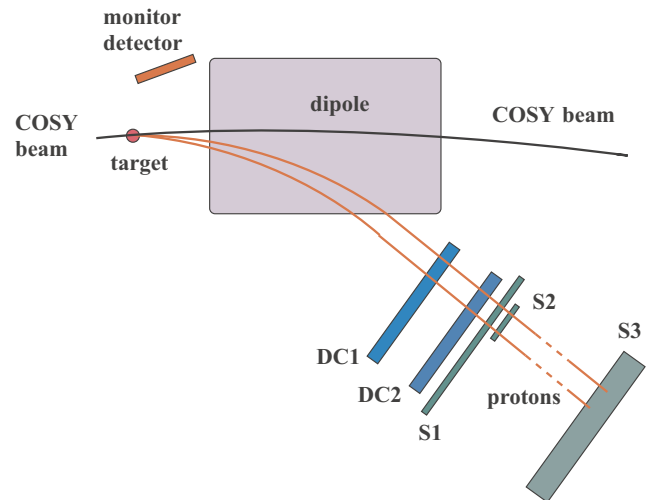

Fig. 1. Sketch of the internal beam facility COSY-11.

be traced back through the magnetic field to the interaction point, leading to a momentum determination. The velocities of these particles are accessible via a time-of-flight path behind the drift chambers, consisting of two scintillation hodoscopes (start detectors S1 and S2) followed by a large scintillation wall (S3) at a distance of ~ 9.3 m, acting as a stop detector. By measuring the momentum and the velocity, particles are identified via invariant mass, *i.e.* the four-momentum vectors P_i of positively charged ejectiles are fully determined.

The event selection for the reaction $pp \to pp\eta'$ was performed by accepting events with two reconstructed tracks in the drift chambers, requiring both particles being identified as protons. The four-momentum determination of the positively charged ejectiles yields a full event reconstruction for the reaction type $pp \to ppX$ and allows an identification of the X-particle using the missing-mass method

$$m_X = |P_{\text{beam}} + P_{\text{target}} - P_{\text{proton1}} - P_{\text{proton2}}| \quad (1)$$

and to study angular distributions of the ejectiles. This situation is demonstrated in fig. 2 for a beam momentum of $p_{\text{beam}} = 3.356$ GeV/c, corresponding to an excess energy of $Q = 46.6$ MeV above the η'-meson production threshold. In the raw spectrum (upper panel) a signal of the η'-meson production is clearly visible on a background arising from multipion production channels. The lower spectrum presents the η' missing-mass peak with a content of $N \sim 13000$ events after subtraction of the background, which was fitted by a first-order polynomial. The observed mean position of the missing-mass peak, $m_X = 958.1$ MeV/c^2, differs by 0.3 MeV/c^2 from the nominal value ($m_{\eta'} = 957.78 \pm 0.14$ MeV/c^2 [38]), reflecting the precision of the experimental method and the quality of the accelerator beam. The missing-mass resolution amounts to $\sigma = 3$ MeV/c^2 ($\Gamma_{\eta'} = 0.202 \pm 0.016$ MeV/c^2 [38]), consistently with Monte Carlo simulations (fig. 2, dashed line) based on GEANT 3.21 [39].

To extract total- and differential-cross-section data, it is important to investigate the phase space coverage of the
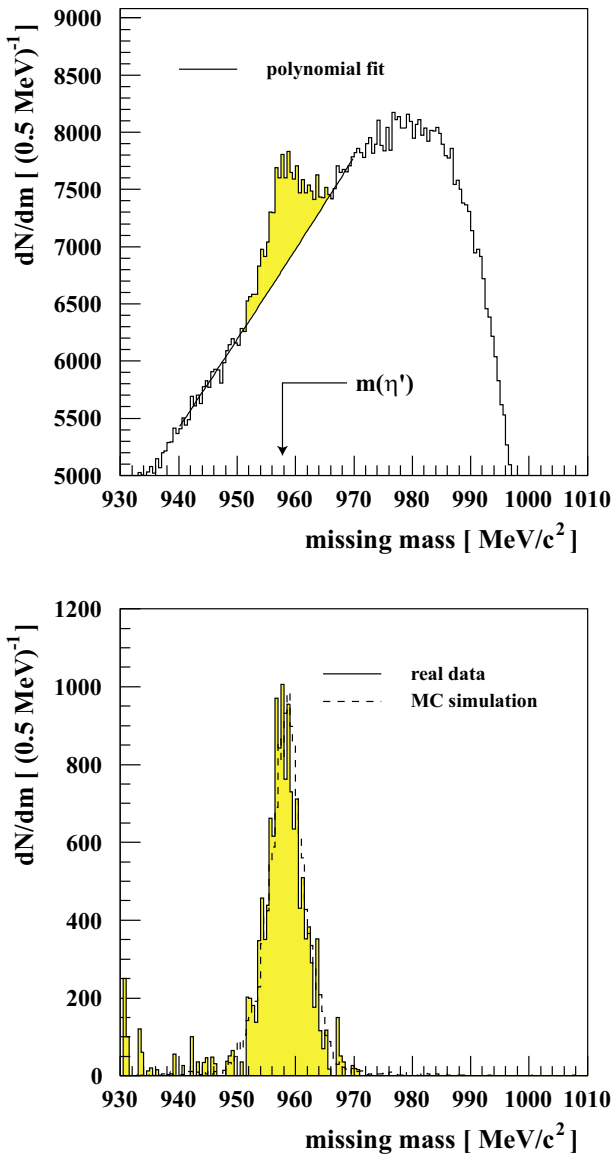
Fig. 2. Missing-mass distribution of the selected two track events with both particles identified as protons ($Q = 46.6$ MeV). The lower panel presents the experimental data after subtraction of the background (see upper panel). In addition, the resulting η' signal (solid line) is compared with expectations according to Monte Carlo simulations (dashed line).

Fig. 3. Dalitz plots for generated (upper panel) and by the COSY-11 detection system accepted (lower panel) Monte Carlo events of the reaction $pp \to pp\eta'$ at an excess energy of $Q = 46.6$ MeV.

detection system. For the highest-energy data point presented in this paper this situation is illustrated in fig. 3 presenting the squared invariant mass of the proton-η' system $S_{p\eta'}$ as a function of the squared invariant mass of the proton-proton system S_{pp} for Monte-Carlo events[1].

As expected, the Dalitz plot displaying all generated events (upper panel) is homogeneously filled, while the corresponding plot for accepted and reconstructed events (lower panel) presents an inhomogeneous structure, re-
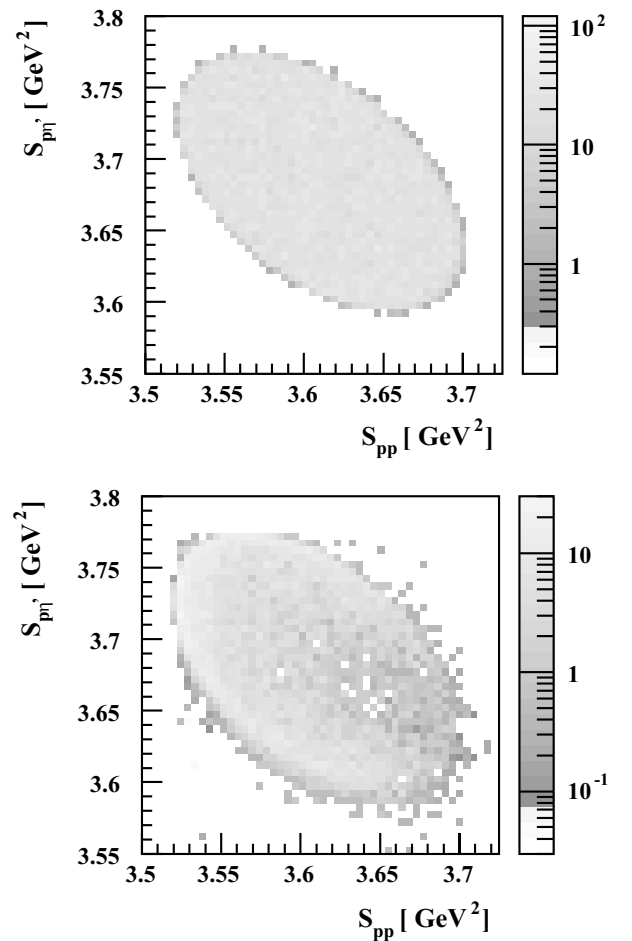
flecting the acceptance of the COSY-11 detection system. However, from the latter spectrum it is obvious that even at an excess energy of $Q = 46.6$ MeV the whole Dalitz plot is covered. The overall detection efficiencies, requiring the detection of both protons, were determined to be

$$\varepsilon(Q = 26.5 \text{ MeV}) = (2.0^{+0.4}_{-0.3}) \times 10^{-2},$$

$$\varepsilon(Q = 32.5 \text{ MeV}) = (1.5^{+0.4}_{-0.3}) \times 10^{-2}, \quad \text{and}$$

$$\varepsilon(Q = 46.6 \text{ MeV}) = (9.2^{+3.2}_{-2.1}) \times 10^{-3}.$$

Especially at high energies the uncertainty in the determination of the detection efficiency is mainly given by the application of different models for the proton-proton FSI [40–44].

To receive an η'-meson angular distribution, the range of scattering angles in the center-of-mass system was divided into eight angular bins and missing-mass spectra have been extracted for each bin. The contents of the missing-mass peaks have been acceptance-corrected by results from phase space Monte Carlo simulations including the pp FSI, according to [40,45]. The inclusion of the

---

[1] The squared invariant mass S_{ij} of two particles i and j with the four-momentum vectors P_i and P_j is given by $S_{ij} = |P_i + P_j|^2$.
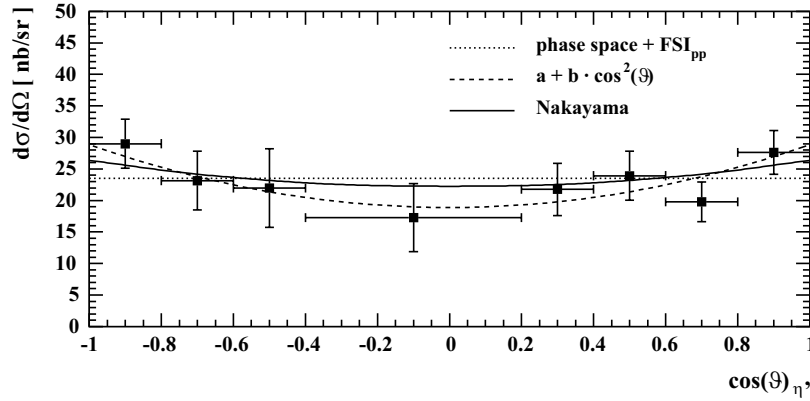
Fig. 4. Angular distribution of the emitted η'-meson in the center-of-mass system at an excess energy of $Q = 46.6$ MeV. Newest results from [48] are represented by the solid line. For comparison, the dashed and the dotted lines indicate expectations according to phase space considerations with and without the inclusion of a $\cos^2(\vartheta)$ term.
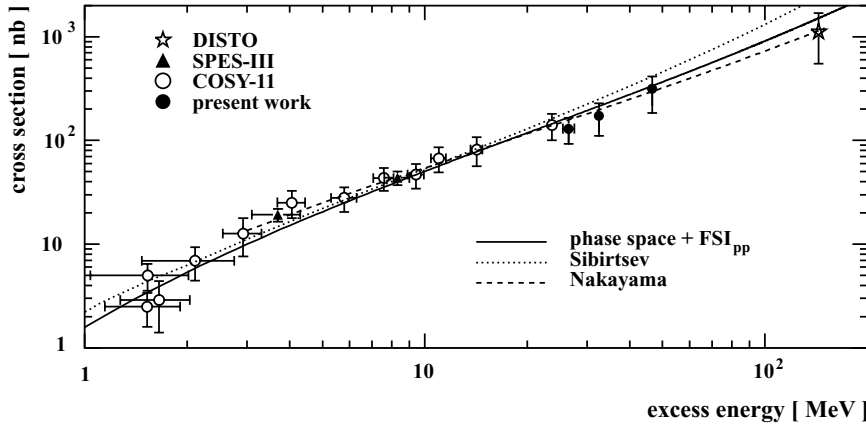

Fig. 5. Total cross-sections for the reaction $pp \to pp\eta'$ as a function of the excess energy Q. Filled circles correspond to the data presented in this paper and triangles, open circles and stars correspond to data from [23–25,46], respectively. The curves are explained in the text.

final-state interaction itself in the event generator is motivated by the use of overall detection efficiencies in the analysis.

3 Results

In fig. 4 the resulting angular distribution of the emitted η'-mesons in the overall center-of-mass system is presented for an excess energy of $Q = 46.6$ MeV. The quoted errors include statistical and systematical errors except contributions from overall systematical uncertainties (*e.g.*, luminosity determination). The differential cross-sections are compatible ($\chi^2 = 0.92$) with an isotropic emission (dotted line), indicating a dominance of S-waves in the final state, consistent with results obtained from the DISTO Collaboration at an excess energy of $Q = 144$ MeV [46]. However, fig. 4 might also indicate contributions of higher partial waves, *i.e.* D-waves. An inclusion of a $\cos^2(\vartheta)$ term to account for higher partial waves leads to an adequate description of the angular distribution as demonstrated by the dashed line ($\chi^2 = 0.45$).

The integrated luminosities have been determined by comparing the differential counting rates of elastically

Table 1. Total cross-sections for the reaction $pp \to pp\eta'$.

Excess energy Q (MeV)	Absolute cross-section σ (nb)
26.5 ± 1.0	130.0 ± 13.8 (stat.) $^{+21.2}_{-24.8}$ (syst.)
32.5 ± 1.0	174.1 ± 20.2 (stat.) $^{+34.3}_{-45.8}$ (syst.)
46.6 ± 1.0	314.9 ± 17.3 (stat.) $^{+81.9}_{-116.5}$ (syst.)

scattered protons with data obtained by the EDDA Collaboration [47]. For beam momenta of $p = 3.292$ GeV/c, 3.311 GeV/c and 3.356 GeV/c, integrated luminosities of $\int L dt = 908$ nb^{-1}, 841 nb^{-1} and 4.50 pb^{-1} (all: $\pm 1\%$ (stat.) $\pm 5\%$ (syst.)) have been determined.

The obtained values of the total cross-sections are listed in table 1. The overall systematical error arises from the detection efficiency determination, the calculation of the luminosity, the uncertainty of the COSY beam momentum ($\Delta p/p \approx 0.1\%$) as well as from acceptance corrections of the differential cross-sections.

In fig. 5 the results (filled circles) are compared with existing data. The solid line represents an *s*-wave phase space calculation (meson production matrix element $|M_0|^2 = \text{const}$) modified by the proton-proton final-state interaction (FSI) and Coulomb effects, scaled to fit the data [28]:

$$\sigma \propto \int_0^{q_{\text{max}}} k_{NN} q^2 |M_0|^2 \cdot |M_{\text{FSI,Coulomb}}|^2 \mathrm{d}q. \qquad (2)$$

In this notation q and k_{NN} represent the momentum of the meson in the CMS and the momentum of either nucleon in the rest frame of the NN subsystem. Within the experimental errors this fit is able to describe the whole set of existent data. Therefore, one can conclude that no further assumptions like a significant η'-proton final-state interaction are needed in order to describe the excitation function. In particular, distinct effects of higher partial waves can be rejected due to the isotropy of the presented angular distribution and the one from DISTO at $Q = 144$ MeV [46].

The dotted curve of fig. 5 represents calculations from Sibirtsev *et al.* [31] based on a one-pion exchange diagram including the pp final-state interaction. While for excess energies below $Q = 25$ MeV the observed excitation function is described well, the new data from COSY-11 (filled circles) as well as the cross-section from DISTO are somewhat overestimated.

Additionally, fig. 4 and fig. 5 show the newest calculation from Nakayama [48] for the near-threshold η'-meson production in proton-proton collisions (dashed lines), based on a relativistic meson exchange model. Since the relative strengths as well as the absolute scales of the considered mesonic, nucleonic and nucleon resonance currents are not known, different combinations reproducing the available total cross-sections are possible. However, in a combined analysis of the η'-meson production in pp and γp interactions Nakayama succeeded in describing both reactions within his model consistently [48]. In this approach the contribution of the mesonic exchange current has been fixed by the photoproduction data and appeared to be much smaller than assumed in earlier calculations [33]. On the contrary, contributions of at least an S_{11} nucleon resonance in the mass region of 1650 MeV/c^2 and probably a P_{11}-resonance in the mass region of 1880 MeV/c^2 were found to be necessary in order to describe the energy dependence of the total cross-sections of both the γp an pp data. Furthermore, in proton-proton collisions contributions of the nucleonic exchange current were estimated to be comparatively small in order to describe within the given uncertainties both the excitation function a well as the observed angular distributions of emitted η'-mesons presented in [46] and in this work (fig. 4).

4 Summary

At the COSY-11 facility the near-threshold η'-meson production in the reaction channel $pp \to pp\eta'$ has been studied at excess energies of $Q = 26.5$, 32.5 and 46.6 MeV. The obtained total-cross-section data fill the region of intermediate excess energies between the low-energy data [23–27] and one data point at a high excess energy [46]. It was demonstrated that within the quoted errors the complete available excitation function can be adequately described by calculations on the basis of the three-body phase space behaviour including effects of the pp FSI only, and no distinct contributions from the η'-proton interaction or higher partial waves are necessary for the interpretation of the data.

A comparison of the data with a pion exchange model calculation from Sibirtsev *et al.* [31] results in an overestimation of the data presented in this paper. This observation is in agreement with the results from DISTO [46] at an excess energy of $Q = 144$ MeV.

Newest calculations of Nakayama [48], based on a relativistic meson exchange model, succeed in describing both the available total-cross-section data as well as the observed angular distribution of emitted η'-mesons. The necessity to consider contributions from nucleon resonance currents in order to describe the observed data might be interpreted as a signal for the role of nucleon resonances for the η' production, similarly to the η-meson case but on a lower scale.

References

1. N. Isgur, Phys. Rev. D **13**, 122 (1976).
2. A. Kazi *et al.*, Nuovo Cimento Lett. **15**, 120 (1976).
3. D.I. Diakonov, M.I. Eides, Sov. Phys. JETP **54**, 232 (1981).
4. J.F. Donoghue *et al.*, Phys. Rev. Lett. **55**, 2766 (1985); E.P. Venugopal, B.R. Holstein, Phys. Rev. D **57**, 4397 (1998).
5. F.J. Gilman, R. Kauffmann, Phys. Rev. D **36**, 2761 (1987).
6. J. Schechter *et al.*, Phys. Rev. D **48**, 339 (1993).
7. P. Ball *et al.*, Phys. Lett. B **365**, 367 (1996).
8. R. Jakob *et al.*, J. Phys. G **22**, 45 (1996).
9. A. Bramon *et al.*, Phys. Lett. B **403**, 339 (1997); Eur. Phys. J. C **7**, 271 (1999).
10. L. Burakovsky, T. Goldmann, Phys. Lett. B **427**, 361 (1998).
11. Fu-Guang Cao, A.I. Signal, Phys. Rev. D **60**, 114012 (1999).
12. C. McNeile, C. Michael, hep-lat/0006020 (2000).
13. I. Halperin, A. Zhitnitsky, Phys. Rev. D **56**, 7247 (1997).
14. H.Y. Cheng, B. Tseng, Phys. Lett. **415**, 263 (1997).
15. D. Atwood, A. Soni, Phys. Lett. B **405**, 150 (1997); W.-S. Hou, B. Tseng, Phys. Rev. Lett. **80**, 434 (1998).
16. N. Nikolaev, COSY NEWS No. 3, published by the Forschungszentrum Jülich in Cooperation with CANU (1998) p. 4.

17. T. Feldmann, Int. J. Mod. Phys. A **15**, 159 (2000).
18. S.D. Bass, e-Print Archive hep-ph/0006348.
19. S.D. Bass, Phys. Lett. B **463**, 286 (1999).
20. G. 't Hooft, Phys. Rev. Lett. **37**, 8 (1976); Phys. Rep. **142**, 357 (1986).
21. S.D. Bass, Nucl. Phys. A **686**, 429 (2001).
22. P. Moskal, e-Print Archive nucl-ex/0110001.
23. F. Hibou *et al.*, Phys. Lett. B **438**, 41 (1998).
24. P. Moskal *et al.*, Phys. Rev. Lett. **80**, 3202 (1998).
25. P. Moskal *et al.*, Phys. Lett. B **474**, 416 (2000).
26. P. Moskal *et al.*, Phys. Lett. B **482**, 356 (2000).
27. Y. Bedfer *et al.*, Acta Phys. Pol. B **29**, 2973 (1998).
28. P. Moskal, M. Wolke, A. Khoukaz, W. Oelert, Prog. Part. Nucl. Phys. **49**, 1 (2002).
29. G. Fäldt *et al.*, Phys. Scr. **T99**, 146 (2002).
30. H. Machner, J. Haidenbauer, J. Phys. G **25** , R231 (1999).
31. A. Sibirtsev, W. Cassing, Eur. Phys. J. A **2**, 333 (1998).
32. C. Hanhart, K. Nakayama, Phys. Lett. B **454**, 176 (1999).
33. K. Nakayama *et al.*, Phys. Rev. C **61**, 024001 (1999).
34. R. Plötzke *et al.*, Phys. Lett. B **444**, 555 (1998).
35. S. Brauksiepe *et al.*, Nucl. Instrum. Methods A **376**, 397 (1996).
36. U. Bechstedt *et al.*, Nucl. Instrum. Methods B **113**, 26 (1996); R. Maier, Nucl. Instrum. Methods A **390**, 1 (1997).
37. H. Dombrowski *et al.*, Nucl. Instrum. Methods A **386**, 228 (1997).
38. K. Hagiwara *et al.*, Phys. Rev. D **66**, 010001 (2002).
39. GEANT-detector Description and Simulation Tool, CERN Program Library Long Writeup W5013, CERN, 1211 Geneva 23, Switzerland (1993).
40. B.L. Druzhinin, A.E. Kudryavtsev, V.E. Tarasov, Z. Phys. A **359**, 205 (1997).
41. B.J. Morton, Phys. Rev. **169**, 825 (1968).
42. J.P. Naisse, Nucl. Phys. A **278**, 506 (1977).
43. H.P. Noyes, H.M. Lipinski, Phys. Rev. C **4**, 995 (1971).
44. H.P. Noyes, Annu. Rev. Sci. **22**, 465 (1972).
45. V. Baru *et al.*, Phys. At. Nucl. **64**, 579 (2001).
46. F. Balestra *et al.*, Phys. Lett. B **491**, 29 (2000).
47. D. Albers *et al.*, Phys. Rev. Lett. **78**, 1652 (1997).
48. K. Nakayama, H. Haberzettl, private communication, e-Print Archive nucl-th/0401030.